Chin. J. Astron. Astrophys. Vol. 4 (2004), No. 6, 507–517
(http://www.chjaa.org or http://chjaa.bao.ac.cn)

Chinese Journal of Astronomy and Astrophysics

Pairwise Velocity Statistics of Dark Halos *

Hai-Yan Zhang[1] and Yi-Peng Jing[2]

[1] Department of Astronomy, Peking University, Beijing, 100871; proudzhy@126.com
[2] Shanghai Astronomy Observatory, the Partner Group of MPI für Astrophysik, Nandan Road 80, Shanghai, 200030

Received 2004 March 14; accepted 2004 May 13

Abstract We have accurately evaluated the halo pairwise velocity dispersion and the halo mean streaming velocity in the LCDM model (the flat $\omega_0 = 0.3$ model) using a set of high-resolution N-body simulations. Based on the simulation results, we have developed a model for the pairwise velocity dispersion of halos. Our model agrees with the simulation results over all scales we studied. We have also tested the model of Sheth et al. for the mean streaming motion of halos derived from the pair-conservation equation. We found that their model reproduces the simulation data very well on large scale, but under-predicts the streaming motion on scales $r < 10\,h^{-1}$ Mpc. We have introduced an empirical relation to improve their model. These improved models are useful for predicting the redshift correlation functions and the redshift power spectrum of galaxies if the halo occupation number model, e.g. the cluster weighted model, is given for the galaxies.

Key words: cosmology: theory — dark matter halo — large-scale structure of universe

1 INTRODUCTION

The power spectrum of the dark matter distribution contains a wealth of information on the cosmological parameters. It is usually measured from redshift surveys of galaxies. In a redshift survey, the spatial distribution of galaxies is distorted by the peculiar velocity of the galaxies. A statistically isotropic distribution of galaxies in real space becomes anisotropic in the redshift space (Geller & Peebles 1973; Davis & Peebles 1983; Kaiser 1987). This effect is manifested in the measurable two-point correlation or power spectrum, and has been widely used to provide information on the dynamics of the universe, i.e. the density parameter and the amplitude of the primordial power spectrum. The theory of the redshift distortion in the linear regime is well understood. The redshift power spectrum $P_{\rm l}^{\rm S}(k,\mu)$ is related to the real space power spectrum $P_{\rm l}^{\rm R}(k)$ by a simple relation (Kaiser 1987)

$$P_{\rm l}^{\rm S}(k,\mu) \equiv P_{\rm l}^{\rm R}(k)[1+\beta\mu^2]^2\,, \tag{1}$$

where μ is the cosine of the angle between the line of sight and the k vector, $\beta = \Omega^{0.6}/b$, Ω the density parameter, and b the linear bias.

* Supported by the National Natural Science Foundation of China.

While the theory in the linear regime is simple and clean, it is still challenging to measure this quantity with available redshift surveys (including SDSS, see Tegmark et al. 2003). This is because on the scales where the distortion can be measured with current surveys, the non-linear effects of bias and motion are already significant (Jing & Börner 2001a). This calls for a non-linear model for the redshift distortion. Although N-body simulations are a dispensable tool for studying the non-linear redshift distortion, the halo model, which assumes an occupation number of galaxies within halos, can also be used to derive the spatial distribution of galaxies in real space or in redshift space (Jing, Mo & Börner 1998). On the basis of the halo model, the correlation function can be written as the sum of two terms. One is essentially described by linear theory and dominates on large scales. The other is inherently non-linear, and dominates on small scales (Seljak 2000; Peacock & Smith 2000; Scoccimarro et al. 2001). Similarly, the redshift power spectrum can be written as a sum of a linear and a non-linear parts (Kang et al. 2002).

Using N-body simulations, Kang et al. (2002) tested the non-linear redshift power spectrum of dark matter predicted by the halo model. They found that the halo model prediction of the redshift distortion is accurate only when the pairwise velocity dispersion (PVD) of halos is accurately known. In this paper, we will carefully investigate the PVD of halos in simulations as a function of the halo mass and redshifts, and will provide an accurate recipe for modeling this quantity. We will also study the mean streaming velocity of halos that is another important quantity for the halo model.

The rest of the paper is arranged as follows. In Section 2 we describe the N-body simulations used in this paper. In Section 3 and Section 4, we construct the models for the halo PVD and the mean halo streaming velocity, respectively. Our main results are summarized in the last section.

2 N-BODY SIMULATION

We first measure the PVD of halos and the halo mean streaming velocity in simulations. The cosmological model has the density parameter $\Omega_0 = 0.3$, the cosmological constant $\Lambda_0 = 0.7$, and the Hubble constant $h = 0.7$ (in units of 100 km s^{-1} Mpc^{-1}). The amplitude σ_8 of the linear power spectrum, which is defined as the rms density fluctuation within an $8\,h^{-1}$ Mpc sphere, is 0.9. Each simulation has 512^3 particles, and is performed using a P^{3}M code with the gravitational softening length of $\epsilon = 30\,h^{-1}$ kpc. The boxsize is $300\,h^{-1}$ Mpc, sufficiently large for this study. We have four independent realizations that differ only in the phase of the initial density fluctuations. For details of the simulations, we refer readers to Jing (2002) and Jing & Suto (2002).

We identify the dark matter halos using the standard friends-of-friends algorithm with the linking parameter $b = 0.2$. We set the minimum mass of the halos as $8.3 \times 10^{11}\,h^{-1}\,M_\odot$, which corresponds to the mass of 50 simulation particles.

The PVD of halos, $\sigma_{12}^{\rm h}(r)$, is obtained by averaging the expression $[(\boldsymbol{v}_1 - \boldsymbol{v}_2)\cdot\boldsymbol{r}/r]^2$ over all pairs of halos in a particular mass range at a fixed separation $r = |\boldsymbol{r}_1 - \boldsymbol{r}_2|$. The same for the halo mean streaming velocity except that the expression is $(\boldsymbol{v}_1 - \boldsymbol{v}_2)\cdot\boldsymbol{r}/r$. Here $\boldsymbol{v}_i$ and $\boldsymbol{r}_i$ are the peculiar velocity and position of i-th halo, respectively. Our simulation results are presented in Fig. 1 and Fig. 3, where the error bars are given by averaging over the four realizations. In the following sections, analytical models are constructed to match these simulation results.

3 THE HALO PAIRWISE VELOCITY DISPERSION (PVD)

3.1 The Model

Following Sheth et al. (2001a), we derive the expression for the PVD of halos. According to the definition, the PVD of halos can be written as follows,

$$\sigma_{12}^{\rm h}(r) = \int\int {\rm d}m_1{\rm d}m_2 \frac{1+\xi_{\rm hh}(m_1,m_2\mid r)}{\Xi_{\rm hh}(r)} \times n(m_1)n(m_2)H(m_1,m_2\mid r)\,, \tag{2}$$

where $\xi_{\rm hh}$ is the two-point correlation function of halos, and $\Xi_{\rm hh} \equiv \int\int {\rm d}m_1{\rm d}m_2 n(m_1)n(m_2)[1+\xi_{\rm hh}(m_1,m_2\mid r)]$. $H(m_1,m_2\mid r)$ is given by

$$H(m_1,m_2\mid r) = \sigma^2_{\rm halo}(m_1) + \sigma^2_{\rm halo}(m_2) - 2\Psi(m_1,m_2\mid r), \tag{3}$$

where $\sigma_{\rm halo}(m)$ is the (one-point) velocity dispersion of halos of mass m in one dimension, and $\Psi(m_1,m_2\mid r)$ is the velocity correlation function of halos along the connecting line between the two halos. The one-point velocity dispersion of halos can be estimated according to the peak theory of Bardeen et al. (1986). For a Gaussian density fluctuation, the peculiar velocity field is statistically isotropic and Gaussian, and its three-dimensional dispersion smoothed over a scale of $R(m)$, $R(m) = \sqrt[3]{3m/4\pi\rho_0}$, is given by

$$\sigma_{\rm v}(m,a) = Haf(a)\sigma_{-1}(m,a)\,, \tag{4}$$

where a is the cosmic scale factor, H is the hubble parameter at time a, $f(a) = \partial\,{\rm ln}D/\partial\,{\rm ln}a$, and σ_j is defined for any integer j as

$$\sigma_j^2(m) = \frac{1}{2\pi^2}\int {\rm d}k k^{2+2j}P(k)W^2[kR(m)]\,, \tag{5}$$

where $W(x)$ is the Fourier transform of the smoothing window, and $P(k)$ is the the linear matter power spectrum. Throughout this paper, we use the real space top-hat window function,

$$W(x) \equiv (3/x^3)[\sin(x) - x\cos(x)]. \tag{6}$$

As Bardeen et al. (1986) showed, the rms peculiar velocity $\sigma_{\rm p}(m)$ of density peaks differs systematically from that of random patches $\sigma_{\rm v}$ by a factor $C(m)$,

$$\sigma_{\rm p}(m) = \sigma_{\rm v}(m)C(m) = \sigma_{\rm v}(m)\sqrt{1-\sigma_0^4/\sigma_1^2\sigma_{-1}^2}\,. \tag{7}$$

Note that this expression does not depend on the height of the peaks. Because $C(m)$ is smaller than 1, the above equation indicates that peaks have slightly lower rms velocities than random patches.

In Eq. (3) above, $\Psi(m_1,m_2\mid r)$ describes the velocity correlation of two halos, as their velocities are modulated by long wave fluctuations. The velocity correlation between two patches of different sizes, along the line connecting them, is

$$\psi(m_1,m_2\mid r) \equiv H^2a^2f^2(a)\int \frac{{\rm d}k}{2\pi^2}P(k)W(k\mid m_1,m_2)K(kr)\,, \tag{8}$$

where $W(k\mid m_1,m_2) \equiv W[kR(m_1)]W[kR(m_2)]$, and the Ws are the Fourier transforms of the top-hat window function, and $K(x) = \sin(x)/x - (2/x^3)[\sin(x) - x\cos(x)]$. We should stress

that this expression is valid for two patches separated by r rather than for peaks. A simply way to generalize the above expression to peaks is to multiply by the appropriate peak constraint factors $C(m)$:

$$\Psi(m_1, m_2 \mid r) \approx C(m_1)C(m_2)\psi(m_1, m_2 \mid r)\,. \tag{9}$$

This is equivalent to assuming that the normalized velocity correlations are the same between the patches and the peaks. Assuming that the halos are formed at the peaks, Sheth et al. (2001a) predicted for the PVD of halos using the above expressions. Now we compare the model predictions with our simulation results in Fig. 1. The model predictions are plotted as the dashed lines. The figure clearly shows that the model significantly underestimates the PVD of halos.

3.2 The Density Dependence of the Halo Velocity Dispersions

Here we consider to improve the model on the PVD of halos, by generalizing the argument of Hamana et al. (2003), for one-point velocity dispersion of halos, to pairwise velocity dispersion of halos. As Sheth & Diaferio (2001) pointed out, the evolution of the halo peculiar velocity depends on the local matter density. Hamana et al. (2003) thus constructed a model for the dependence of the (one-point) halo peculiar velocity dispersion, $\sigma^2_{\rm halo}(m, \delta)$, on the local background density δ.

The dependence of the halo peculiar velocity on the local density is parameterized as (Hamana et al. 2003),

$$\sigma^2_{\rm halo}(m, \delta) = [1 + \delta(R_{\rm local})]^{2\mu(R_{\rm local})}\sigma^2_{\rm p}(m)\,, \tag{10}$$

where $R_{\rm loccal}$ is the smoothing scale that defines the local background density δ. The key question is how to define the appropriate smoothing length scale. Evidently, $R_{\rm loccal}$ should enclose the gravitational coherence scale which is responsible for the local deviation of the peculiar motion of halos from its global value (for instance, given by linear theory). In their paper, they adopted an ansatz that $R_{\rm loccal}$ is given by a relation of the form $\sigma_0(R_{\rm loccal}) = \sigma_{\rm local}$, and determine the model parameter $\sigma_{\rm local}$ empirically using N-body simulations. They found that choosing $\mu = 0.5$ with $R_{\rm local}$ given by $\sigma_{\rm local} = 0.3$ provides reasonable fits to the results of N-body simulations.

We denote by $p(m \mid \delta)$ the probability of finding a halo with mass m in a region with background density δ. Then the peculiar velocity dispersion of halos with mass m is given by summing up the dispersion $\sigma^2_{\rm halo}(m, \delta)$ weighted by the probability:

$$\sigma^2_{\rm halo}(m) = \frac{\int {\rm d}\delta p(m \mid \delta)\sigma^2_{\rm halo}(m, \delta)}{\int {\rm d}\delta p(m \mid \delta)}\,. \tag{11}$$

We use the linear bias model (Sheth & Tormen 1999) $p(m \mid \delta) = [1 + b(m)\delta]p_{\rm dm}(\delta)$ and the log-normal model for the probability distribution function of dark matter $p_{\rm dm}(\delta)$ (Kayo, Taruya & Suto 2001) to compute $\sigma^2_{\rm halo}(m)$. As shown by Hamana et al., the above calculated $\sigma^2_{\rm halo}(m)$ agrees with the one-point velocity dispersion of halos in N-body simulations.

When we generalize the above argument to the PVD of halos, it is clear that $\sigma^2_{\rm halo}(m)$ in Eq. (3) should be replaced with Eq. (11). However, we have two options to modify the velocity correlation function Eq. (9). One is to replace $C(m)$ in Eq. (9) with $\sigma_{\rm halo}(m)/\sigma_{\rm v}(m)$, and the other is to leave the expression unchanged as Eq. (9). The results calculated with these two options are plotted in Fig. 1 with dotted and solid lines, respectively. Comparing with our

N-body simulation results, we find that the model with the latter option is much more accurate on separation larger than $\sim 3\,h^{-1}$ Mpc (on the smaller scales, nonlinear effects will play an important role which will be considered in the next section). Including the density dependence of the one-point halo velocity dispersion greatly improves the agreement of the model with the simulation at large scales. The decrease of the halo PVD with the separation can be accurately accounted for by the velocity correlation of halos given by Eq. (9). The density dependence should be considered for the one-point velocity dispersion of halos, but not for the correlation of the halo velocities. A plausible explanation for this apparent inconsistency is that the local density field affects the velocity of two nearby halos similarly, so the velocity correlation that depends on the relative velocity of two halos is much less affected by the local density. On separation larger than $\sim 3\,h^{-1}$ Mpc, the model prediction for the halo PVD agrees with the simulation results typically to within 10%. On the smaller scales, the non-linear effects are important, and we evaluate the scale dependence on the small scales using an empirical approach.

3.3 An Empirical Model for the Scale Dependence on Small Scales

On scales smaller than $\sim 3\,h^{-1}$ Mpc, the non-linear effects start to play an important role in altering the predictions of linear perturbation theories. For example, dynamical frictions can reduce the PVD of halos when a pair of halos approach each other. The non-linear effects are complicated to model, so here we present an empirical relation which can greatly improve the agreement between the model and the simulation results on small scales. It reads,

$$\Sigma_{12}^{\rm h}(r) = \sigma_{12}^{\rm h}(r) \times \frac{1}{1+(\frac{2R}{r})^2}\ , \tag{12}$$

where $R = \sqrt[3]{3m/800\pi\rho_0}$ is the radius of the halos. Putting all together, the solid lines in Fig. 2 show our model prediction that uses Eq. (11) for the one-point velocity dispersion of halos, Eq. (9) for the velocity correlation, and Eq. (12) for correcting for the non-linear effects on the small scales. The model shows a very good agreement with the simulation results of halo PVD on all scales.

4 THE HALO MEAN STREAMING MOTION

We begin this section by introducing a model for the mean streaming motion of dark matter, and in Subsection 4.2 we extend it to the halos and compare the model with our simulation results. The derivation follows the work of Sheth et al. (2001b).

4.1 The Dark Matter

The mean streaming velocity of dark matter can be obtained according to the pair-conservation equation (Peebles 1980). It usually can be written as,

$$\frac{\partial(1+\bar{\xi}(r))}{\partial \ln a} = -\frac{v_{12}(r)}{Hr} 3[1+\xi(r)]\,, \tag{13}$$

where $\bar{\xi}(r)$ is the volume-averaged correlation function over a ball of proper separation. On the large separation that is of interest to us here, the linear approximation $\bar{\xi}(r,a) = [D(a)/D_0]^2\bar{\xi}(r,a_0)$ is valid for the evolution of $\bar{\xi}(r,a)$, where $D(a)$ is the linear theory growth factor at a, and D_0

is the present value of $D(a)$. With this approximation, the pair-conservation equation can be written as (Peebles 1980),

$$-\frac{v_{12}(r)}{Hr} = \frac{2}{3}\frac{f(a)\bar{\xi}(r,a)}{1+\xi(r,a)}\,. \tag{14}$$

This approximation is valid only on large scales ($r \geq 5\,h^{-1}$ Mpc) where the linear purterbation theory is valid. It underestimates the exact solution by a factor of 3/2 or so on smaller scales (Juszkiewicz, Springel & Durrer 1999; Sheth et al. 2001a).

4.2 The Halos

Equation (14) cannot be used directly to estimate the streaming motion of halos, because the number of halos is not conserved, nor is the number of halo pairs. However, Sheth et al. (2001b) provided an estimate for the streaming motion of halos, by assuming that every halo is represented by one particle that is at the halo center of mass. Then they imagined tracing these center of mass particles back in time and considered the evolution of their spatial distribution. By definition, these hypothetical particles are neither produced or annihilated during the evolution, therefore, the pair-conservation equation can be used for describing the evolution of these particles.

According to Mo & White(1996), the linear bias factor $b(m)$ of these hypothetical particles is given by

$$b(m,a) = 1 + \frac{\nu^2(m)-1}{\delta_{c0}D(a)/D_0}, \tag{15}$$

where $\nu(m) = \delta_{c0}/\sigma(m)$, and $\delta_{c0} = 1.68$. For this bias factor, we have

$$\frac{\partial b(m,a)}{\partial \ln a} = f(a)[1-b(m,a)]. \tag{16}$$

Since we know the evolution of the two-point correlation function of halos, we can derive the mean streaming motion of halos from the the pair-conservation equation. For a pair of halos with mass m_1 and m_2, their mean streaming motion is (Sheath et al. 2001b)

$$\frac{v_{12}^{\rm h}(r)}{Hr} = \frac{v_{12}^{\rm dm}(r)}{Hr}\frac{b_1b_2[1+\xi_{\rm dm}^{\rm Lin}(r)]}{[1+b_1b_2\xi_{\rm dm}^{\rm Lin}(r)]} - \frac{f(a)\xi_{\rm dm}^{\rm Lin}(r)}{3}\frac{[b_1(1-b_2)+b_2(1-b_1)]}{[1+b_1b_2\xi_{\rm dm}^{\rm Lin}(r)]}, \tag{17}$$

where $b_1 = b(m_1, a=1)$ and $b_2 = b(m_2, a=1)$. If we insert the linear evolution approximation, then this becomes

$$\frac{v_{12}^{\rm h}(r)}{Hr} = \frac{v_{12}^{\rm dm}(r)}{Hr}\Big(\frac{b_1+b_2}{2}\Big)\frac{1+\xi_{\rm dm}^{\rm Lin}(r)}{1+b_1b_2\xi_{\rm dm}^{\rm Lin}(r)}\,. \tag{18}$$

It is easy to see when $b_1 = b_2 = 1$, $v_{12}^{\rm h}(r) = v_{12}^{\rm dm}(r)$. Also, in the large separation limit, $v_{12}^{\rm h}(r) \longrightarrow [(b_1+b_2)/2]v_{12}^{\rm dm}(r)$. Notice that the linear theory and linear evolution approximation we used to obtain Eq. (18) are not accurate on small scales. Nevertheless, this provides us at least some indication of the small-scale behavior of the halo streaming motion.

In fact, when the model is studied in several different halo mass ranges separately, the weighting factor, which is the ratio of the number of m_1 and m_2 halo pairs at r to the total number of halo pairs at r, should be considered. So the halo mean streaming motion can be written as (Sheth et al. 2001b)

$$-\frac{V_{12}^{\rm h}(r)}{Hr} = -\int\int {\rm d}m_1{\rm d}m_2\frac{v_{12}^{\rm h}(r)}{Hr}\times\frac{n(m_1)n(m_2)[1+b(m_1b(m_2)\xi_{\rm dm}^{\rm Lin}(r)]}{\bar{n}_{\rm h}^2+\bar{b}_{\rm h}^2\xi_{\rm dm}^{\rm Lin}(r)}$$

$$= \frac{2f(a)}{3}\frac{\bar{n}_{\rm h}\bar{b}_{\rm h}\bar{\xi}^{\rm Lin}_{\rm dm}(r)}{\bar{n}_h^2 + \bar{b}_{\rm h}^2\xi^{\rm Lin}_{\rm dm}(r)}\,, \tag{19}$$

where $\bar{n}_{\rm h} \equiv \int {\rm d}mn(m)$ is the average number density of halos, and $\bar{b}_{\rm h} \equiv \int {\rm d}mn(m)b(m)$ is their average bias factor. The final expression of Eq. (19) follows from inserting Eq. (18) for $v_{12}^{\rm h}$ and Eq. (14) for $v_{12}^{\rm dm}$.

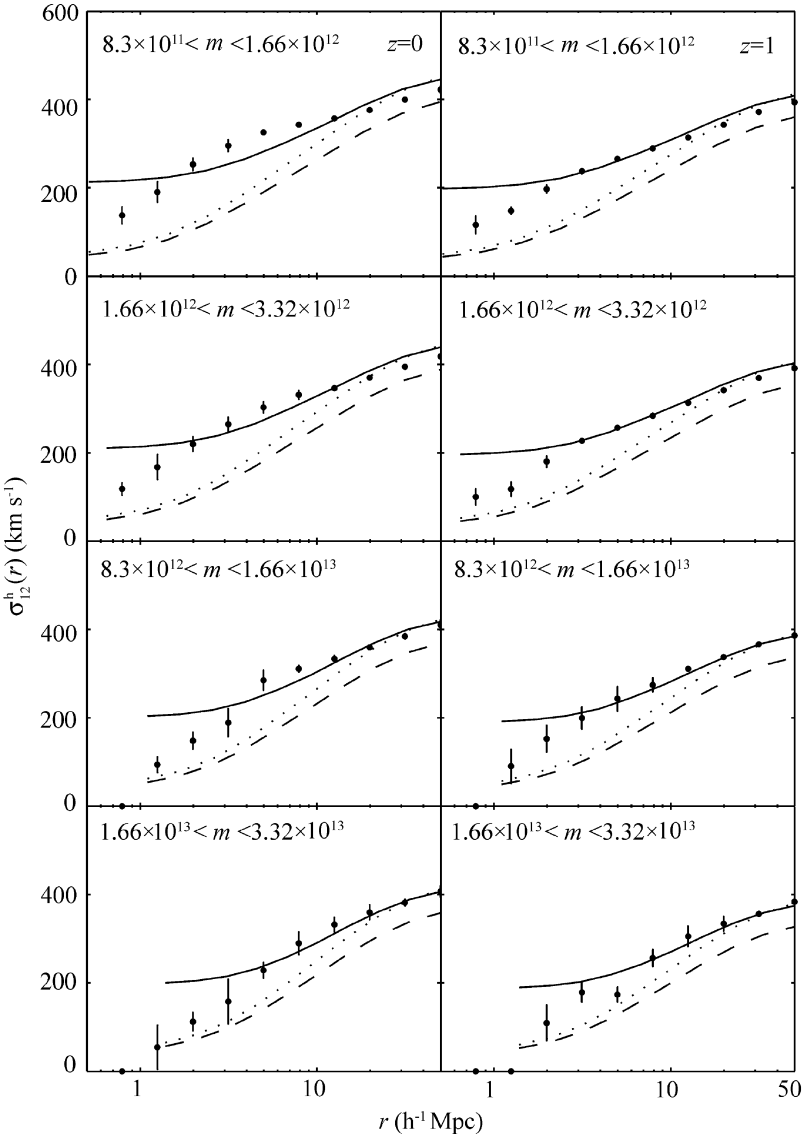

Fig. 1 Pairwise velocity dispersions of halos. Halo mass ranges (in the unit of $h^{-1}\ M_\odot$)are denoted in each plot. Filled circles show the measurements from the simulation. Dashed curves show the prediction based on the peak theory. Dotted curves are the model prediction when the density dependence is considered both for the one-point halo velocity dispersion and similarly for the velocity correlation function. Solid curves show the model prediction with the density dependence correction applied solely to the one-point halo velocity dispersion.

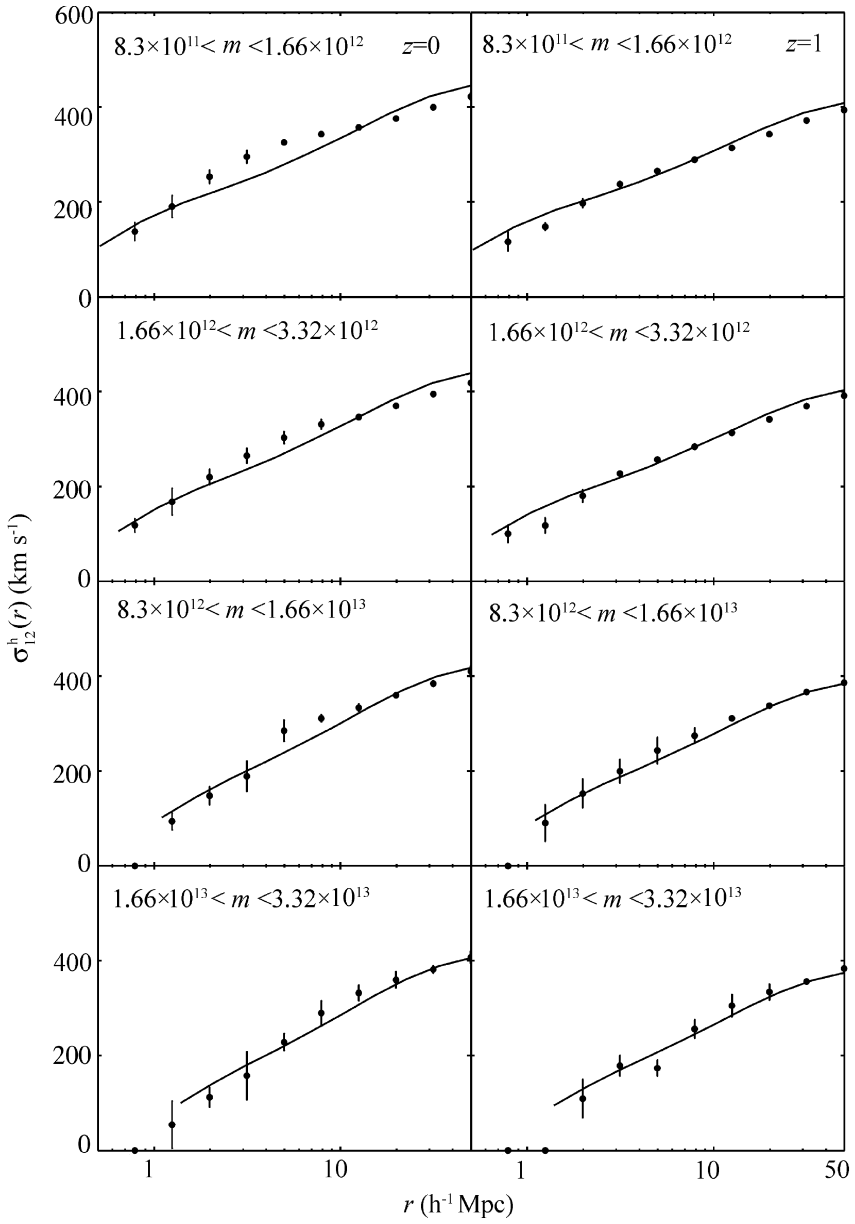

Fig. 2 Pairwise velocity dispersions of halos. Halo mass ranges (in the unit of $h^{-1}\ M_{\odot}$)are denoted in each plot. Filled circles show the measurements of simulations. Solid curves show the predictions of our model based on Eq. (9), Eq. (11), and Eq. (12).

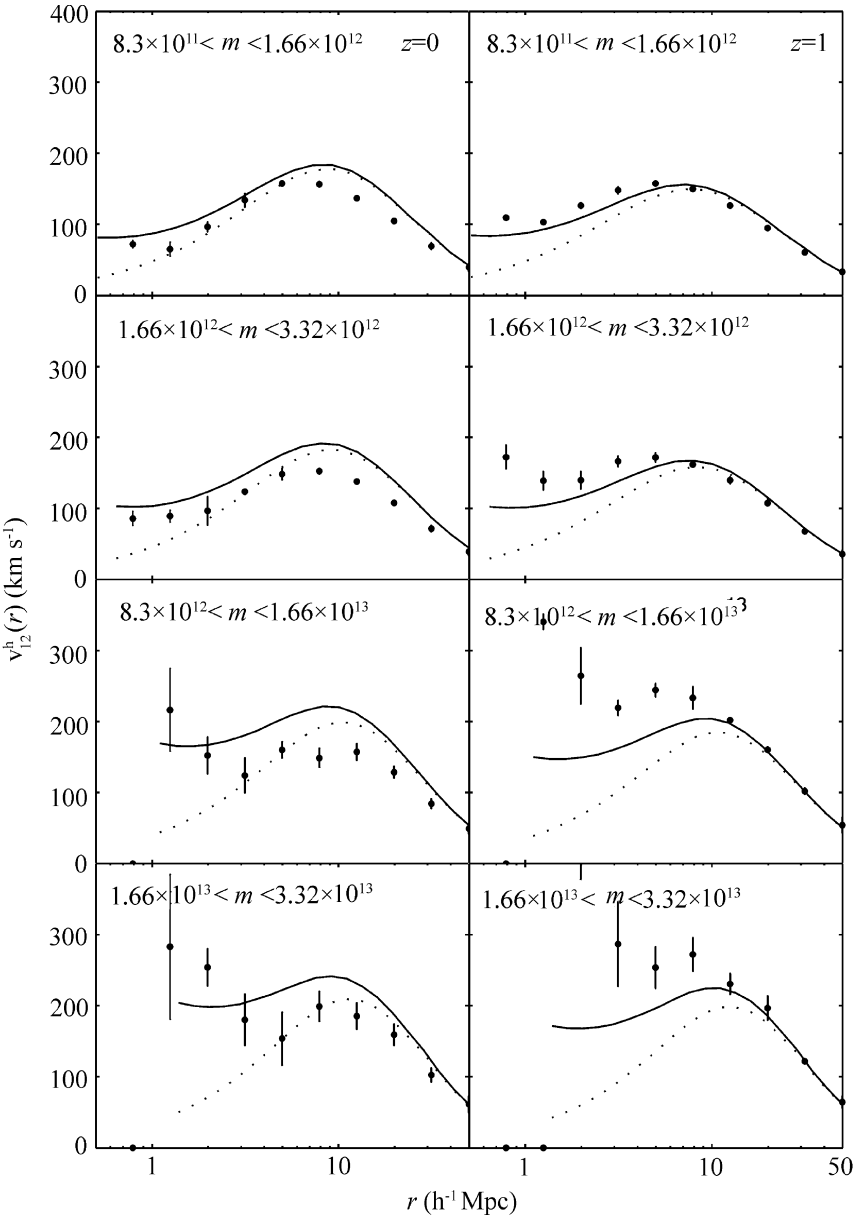

Fig. 3 Mean streaming motions of halos. Halo mass ranges (in the unit of $h^{-1}\ M_{\odot}$) are denoted in each plot. Filled circles show the measurements of simulations. Dotted curves show the predictions for the halos (Eq. (19)). Solid curves are for the empirical correction on small scales (Eq. (20)) .

It should be pointed out that the evolution of the bias factor (Eq. 16) is generally valid even if the bias factor is not Eq. (15), as $b = 1 + b_L$ always holds (Mo & White 1996; Jing 1999; Fan 1999; Sheth & Tormen 1999). Because it was demonstrated that the bias model of Mo & White (1996) underestimates the bias for small mass halos (Jing 1998), we will use the empirical formula of Sheth and Tormen for the bias factor. Figure 3 shows the halo mean streaming velocity in the N-body simulation (filled circles) together with the linear theory prediction Eq. (19) (dotted curves). The model prediction agrees very well with our simulation on large scales. However, on scales less than about 10 times of the halo radius R, the simulation results are higher than the model prediction. The discrepancy increases with decreasing separation. This behavior can be understood in this way. When the hypothetical particles are traced back to early time, these particles are well separated and there are no pairs with separation less than $r_{\rm min}$, i.e., the two-point correlation function of these particles is -1 for $r < r_{\rm min}$. With the evolution, $r_{\rm min}$ becomes smaller as the particles approach each other, and the two-point correlation function develops on the small scales. This evolution of the correlation function has not been included in the above model, which could be the main reason why the model does not agree with the simulation results. It is complicated to follow quantitatively the development of the correlation function of the hypothetical particles on small scales. Again we adopt an empirical relation to account for this phenomenon with the following relation,

$$V^{\rm h}_{12,{\rm c}}(r) = V^{\rm h}_{12}(r) \times \left[1 + (m/m_\star)^{0.1} \left(\frac{4R}{r}\right)^{1.5}\right]. \qquad (20)$$

The solid lines in Fig. 3 are the model predictions with the above correction, which agree better with the simulation results.

5 CONCLUSIONS

We have accurately evaluated the halo pairwise velocity dispersion and the halo mean streaming velocity in the currently popular LCDM model using a set of high-resolution N-body simulations. Following the work of Sheth et al.(2001) and Hamana et al. (2003), we have developed a model for the pairwise velocity dispersion of halos. The model has two ingredients: a halo velocity dispersion and a velocity correlation function. We demonstrated that the density dependence of Hamana et al. should used for the halo one-point velocity dispersion, but not for the velocity correlation. The model thus constructed is a significant improvement over the model originally proposed by Sheth et al. (2001). We further refine the model by introducing an empirical correction factor Eq. (12) for the dependence on small scale.

We have also tested the model for the mean streaming motion of halos derived from the pair-conservation equation. We found that the model reproduces the simulation data very well on large scale, but under-predicts the streaming motion on scales $r < 10R$. The discrepancy is caused by inadequate modeling of the correlation functions of the hypothetical particles on small scales. We have introduced an empirical relation to account for this discrepancy. The corrected model prediction is in good agreement with the N-body results.

The models presented here are accurate despite that some of the model ingredients are empirical. They can be used to predict the redshift correlation functions and the redshift power spectrum of galaxies if the halo occupation number model, e.g., the cluster weighted model, is given for the galaxies.

References

Bardeen J. M., Bond J. R., Kaiser N. et al., 1986, ApJ, 304, 15
Davis M., Peebles P. J. E., 1983, ApJ, 267, 465
Fan Z. H., 2000 ApJ, 528, 585
Geller M. J., Peebles P. J. E., 1973, ApJ, 184, 329
Hamana T., Kayo I., Yoshida N. et al., 2003, MNRAS, 343, 1312
Jing Y. P., 1998 ApJ, 503, L9
Jing Y. P., 1999 ApJ, 515, L45
Jing Y. P., 2002 MNRAS, 335, L89
Jing Y. P., Börner G., 2001, MNRAS, 325, 1389
Jing Y. P., Mo H. J., Börner G., 1998, ApJ, 494, 1
Jing Y. P., Suto Y., 2002, ApJ, 574, 538
Juszkiewicz G., Springel V., Durrer R., 1999, ApJ, S18, L25
Kaiser N., 1987, MNRAS, 227, 1
Kang X., Jing Y. P., Mo H. J. et al., 2002, MNRAS, 336, 892
Kayo I., Taruya A., Suto Y., 2001, ApJ, 561, 22
Mo H. J., White S. D. M., 1996, MNRAS, 282, 347
Peacock J., Smith R., 2000, MNRAS, 318, 1144
Peebles P. J. E., 1980, The Large Scale Structure of the Universe, Princeton: Princeton Univ. Press.
Scoccimarro R., Sheth R. K., Hui L. et al., 2001, ApJ, 546, 20
Seljak U., 2000, MNRAS, 318, 203
Sheth R. K., Diaferio A., 2001, MNRAS, 322, 901
Sheth R. K., Diaferio A., Hui L. et al., 2001b, MNRAS, 326, 463
Sheth R. K., Hui L., Diaferio A. et al., 2001a, MNRAS, 325, 1288
Sheth R. K., Tormen G., 1999, MNRAS, 308, 119
Tegmark M., Blanton M., Strauss M. et al., 2003, preprint (astro-ph/0310725)